

Original Research

# RIPK4 Promotes Cell Invasion and the Epithelial–Mesenchymal Transition in Ovarian Cancer

Li Hua<sup>1,2,†</sup>, Jian-Hai Wu<sup>3,†</sup>, Jing-Ying Xu<sup>2,†</sup>, San-Gang Wu<sup>1,4,\*</sup>, Juan Zhou<sup>1,2,\*</sup><sup>1</sup>The School of Clinical Medicine, Fujian Medical University, 350005 Fuzhou, Fujian, China<sup>2</sup>Department of Obstetrics and Gynecology, The First Affiliated Hospital of Xiamen University, School of Medicine, Xiamen University, 361003 Xiamen, Fujian, China<sup>3</sup>Endoscopy Center, The First Affiliated Hospital of Xiamen University, School of Medicine, Xiamen University, 361003 Xiamen, Fujian, China<sup>4</sup>Department of Radiation Oncology, Xiamen Cancer Center, Xiamen Key Laboratory of Radiation Oncology, The First Affiliated Hospital of Xiamen University, School of Medicine, Xiamen University, 361003 Xiamen, Fujian, China\*Correspondence: [wusg@xmu.edu.cn](mailto:wusg@xmu.edu.cn) (San-Gang Wu); [zhoujuan@xmu.edu.cn](mailto:zhoujuan@xmu.edu.cn) (Juan Zhou)

†These authors contributed equally.

Academic Editor: Mariafrancesca Cascione

Submitted: 24 May 2023 Revised: 10 September 2023 Accepted: 19 September 2023 Published: 29 December 2023

## Abstract

**Objective:** To investigate the clinical role and biological function of receptor-interacting protein kinase 4 (RIPK4) in ovarian cancer (OC). **Methods:** We conducted a comprehensive analysis of the expression and prognostic role of RIPK4 in OC using various public databases including The Cancer Genome Atlas, Oncomine, and Kaplan–Meier plotter. *In vitro* studies included wound healing, cell migration and invasion, cell proliferation, and cell apoptosis assays as well as vascular mimicry experiments. *In vivo* studies were conducted using subcutaneous and intraperitoneal xenografts. **Results:** Our findings revealed that RIPK4 was significantly overexpressed in OC tissue compared to normal ovarian tissue. Moreover, the overexpression of RIPK4 was associated with advanced-stage disease and a poor prognosis in OC patients. RIPK4 silencing resulted in significant inhibition of intraperitoneal tumor growth, invasion, and vascular mimicry in OC cells. Furthermore, downregulation of RIPK4 inhibited the epithelial–mesenchymal transition of OC cells both *in vitro* and *in vivo* by promoting the expression of E-cadherin and inhibiting the expression of N-cadherin. **Conclusion:** The results of this study suggest that RIPK4 may function as an oncogene in the development and prognosis of OC.

**Keywords:** ovarian cancer; RIPK4; EMT; biomarker; prognosis

## 1. Background

Ovarian cancer (OC) is the most lethal malignancy of gynecological tumors, with approximately 90% of patients diagnosed with epithelial OC [1,2]. Due to insidious symptoms, 70% of OC patients are diagnosed at an advanced stage [1]. While survival rates for advanced OC have improved in the past decades [3], approximately 70% of patients experience local or distant recurrence within 3 years after treatment [4]. Therefore, it is critical to explore new diagnostic and therapeutic targets to improve the early detection and prognosis of OC patients.

Receptor-interacting protein kinase 4 (RIPK4) plays a crucial role in maintaining epidermal homeostasis by regulating skin keratinocyte differentiation [5]. Moreover, RIPK4 is associated with the development of various cancers [6]. Knockdown of RIPK4 has been shown to suppress Wnt-dependent xenograft tumor growth in OC cells [7]. However, the precise biological behavior of RIPK4 in OC and the mechanism underlying the development of OC remain unclear.

We hypothesized that RIPK4 may regulate the occurrence and progression of OC by regulating the proliferation, migration, invasion, angiogenesis, and epithelial–

mesenchymal transition (EMT) of OC cells both *in vitro* and *in vivo*. In this study, we investigated the role of RIPK4 in regulating OC development and determined its potential biological function.

## 2. Materials and Methods

### 2.1 Gene Expression Profiling Interactive Analysis Database

The Gene Expression Profiling Interactive Analysis (GEPIA) database (<http://gepia.cancer-pku.cn/>) is a comprehensive platform that collects and integrates the RNA sequencing data of 9736 tumor tissues and 8587 normal tissue samples obtained from The Cancer Genome Atlas (TCGA) and Genotype-Tissue Expression databases. This database allows for the rapid and convenient profiling of gene expression in both tumor and normal tissues [8]. In our study, we used the GEPIA database to validate the differential expression of RIPK4 between OC tissue and normal tissue.  $|\log_2 \text{fold change}| > 1$  and  $p < 0.05$  are considered statistically significant.



## 2.2 Oncomine Database

The Oncomine database (<https://www.oncomine.org>) has a comprehensive collection of 715 datasets, including 86,733 samples from cancer patients. It is the largest cancer research database, providing invaluable support to researchers in identifying differentially expressed genes and potential therapeutic targets [9]. In our study, we used the Oncomine database to compare the expression levels of RIPK4 between different pathological subtypes of OC with normal tissue.

## 2.3 Clinical Specimen Collection

To further identify the differential expression of RIPK4 in OC compared to normal ovarian tissue, we included a total of five patients with FIGO stage III–IV serous OC tissues and three patients with normal ovarian tissues in the analyses. This study was approved by the institutional review board of the First Affiliated Hospital of Xiamen University (No.2021GGB027; Xiamen, China), and written informed consent was obtained from all participating patients.

## 2.4 TCGA Database

TCGA (<https://www.tcgabio.org/>) is a remarkable project created by the National Cancer Institute and the National Human Genome Research Institute. TCGA database has compiled genomics information from 20,000 primary cancers as well as clinical data, diagnosis, treatment, and survival outcomes of patients. This comprehensive platform has facilitated the identification of significant research indicators. In this study, we utilized TCGA database to investigate the relationship between the expression of RIPK4 and clinical characteristics of patients with OC, as well as to examine the impact of RIPK4 on prognosis in detail. Therefore, we downloaded the RNA sequencing results of OC patients as well as their clinical information including age, clinical stage, tumor grade, histological type, lymphatic infiltration, blood metastasis, and survival outcomes.

We employed the receiver operating characteristic (ROC) curve to determine the appropriate cut-off point for RIPK4 mRNA expression in relation to survival outcome. Based on this cut-off point, patients were divided into two groups: high and low expression. We utilized a multivariate Cox proportional hazards risk model to assess the independent risk of RIPK4 on prognosis.

For gene set enrichment analysis (GSEA), we utilized GSEA3.0 software (Broad Institute, SD, USA) and employed the `c2.cp.kegg.v6.symbols.gmt` data set from the Molecular Signatures Database as the functional gene set. Default weighted enrichment statistics were employed, and 1000 random combinations were generated to identify genes with  $p < 0.05$  and false discovery rate  $< 0.05$ . These genes were considered significant and constituted the enriched gene set.

## 2.5 Kaplan–Meier Plotter Database

We utilized the Kaplan–Meier (KM) plotter database (<http://www.kmplot.com/analysis/>) [10], which specializes in KM survival analysis of genes and their impact on the prognosis of patients with different types of cancer. This database compiles and integrates data from various sources, including the Gene Expression Omnibus, European Genome-phenome Archive, and TCGA databases, making up for the limitation of the small sample size of OC patients in TCGA database. Therefore, we employed the KM plotter database to gain further insights into the influence of RIPK4 on the survival of OC patients.

## 2.6 Cell Culture and Transfection

The SKOV3 human ovarian cancer cell line was obtained from the Xiamen University Cancer Center Institute. Cells were cultured in Dulbecco's Modified Eagle Medium (DMEM; Gibco, Brisbane, Australia) supplemented with 10% fetal bovine serum (Cellmax, Beijing, China) and 1% penicillin and streptomycin (RiboBio, Guangzhou, China). The cells were placed in a 5% CO<sub>2</sub> incubator at 37 °C with saturated humidity. To establish an OC model with low RIPK4 expression, 10 μL small interfering RNA (siRNA) targeting RIPK4 (siRIPK4) with chemical modification and 10 μL negative control siRNA (siNC) (GenePharma, Shanghai, China) were transfected into SKOV3 cells at 30–50% confluence. The cells were cultured in a 6-well plate using an siRNA reagent system (Biogen, Shanghai, China) according to the manufacturer's specifications. After incubating for 48 h, the expression of RIPK4 was assessed by quantitative PCR (qPCR), western blotting (WB), and immunofluorescence staining. Subsequent experiments were conducted to examine the impact of RIPK4 on the biological behaviors of OC cells. The sequences of siRIPK4 and negative control siRNA are summarized in **Supplementary Table 1**. The cell line was verified by short tandem repeat DNA profiling, and confirmed to be free of Mycoplasma species.

## 2.7 Quantitative PCR (qPCR)

Total RNA was isolated using TRIzol reagent (Applygen, Beijing, China). Reverse transcription was performed using the HisScript II RT SuperMix for qPCR (Vazyme Biotech Co., Ltd., Nanjing, China) according to the manufacturer's instructions. The qPCR assay was conducted using the Hieff qPCR SYBR reagent (Yeasen Biotechnology, Shanghai, China) in a total volume of 20 μL on the ABI 7500 Quantitative PCR System (Applied Biosystems, Foster City, CA, USA) under the following conditions: 50 °C for 5 min, 95 °C for 5 min, followed by 40 cycles of 95 °C for 10 s and 60 °C for 31 s, and a final extension step of 95 °C for 15 s and 60 °C for 1 min. The relative expression of other genes, with GAPDH as the reference, was calculated using the  $2^{-\Delta\Delta C_t}$  method, and all experiments

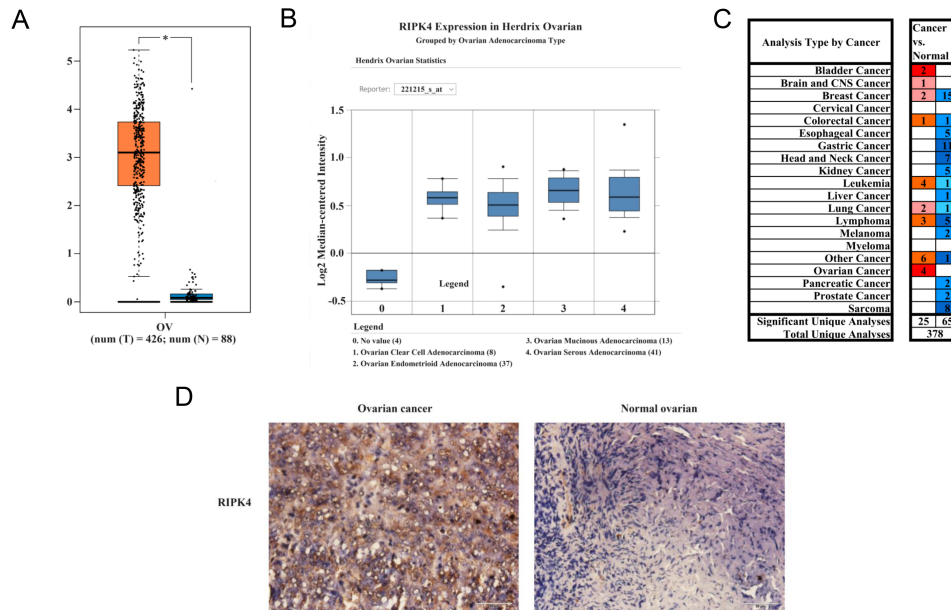


**Fig. 1. The differentially expressed genes were obtained from databases and tissues.** (A) Gene Expression Profiling Interactive Analysis (GEPIA) database. (B) OncoPrint database. (C) The expression of receptor-interacting protein kinase 4 (RIPK4) in various cancers and normal tissue from the OncoPrint database (blue represents low expression in cancers and red represents high expression in cancers). The deep color indicates ranking at the top. (D) Immunohistochemical staining of RIPK4 in ovarian cancer (OC) and normal ovarian tissues (magnification, 40 $\times$ ). The data are presented as the mean  $\pm$  standard deviation (SD), and statistical significance is indicated as follows: \* $p < 0.05$ .

were performed in triplicate under the same conditions. The primer sequences used in this study are summarized in **Supplementary Table 1**.

### 2.8 Western Blotting (WB)

Total protein was isolated using moderate-strength RIPA buffer containing 2% protease inhibitors and 1% phosphoprotein inhibitors (Applygen). The lysates were centrifuged at 12,000 rpm for 15 min at 4  $^{\circ}$ C. The resulting supernatant was transferred to new 1.5 mL Eppendorf tubes. Protein concentration was measured using a BCA protein assay kit (Abcam, Cambridge, MA, USA). RIPA buffer and 5 $\times$  loading buffer were used to normalize the protein concentrations. Then the mixture was boiled for 10 min. A total of 20  $\mu$ g protein was loaded onto a 5% sodium dodecyl sulfate–polyacrylamide gel electrophoresis (SDS-PAGE) gel and concentrated for approximately 40 min, followed by separation on a 10% SDS-PAGE gel for approximately 60 min. The targeted proteins in the separated gel were electrotransferred onto PVDF membranes (Millipore, Burlington, MA, USA). The membranes were blocked in 5% BSA (Solarbio, Beijing, China) for 1.5 h, followed by overnight incubation with primary antibody at 4  $^{\circ}$ C. Then the PVDF membranes were washed with 10% Tris-buffered saline with 0.1% Tween $^{\circ}$  20 detergent (TBST), incubated

with secondary mouse or rabbit antibody for 1 h, and then washed again with 10% TBST. Finally, an enhanced chemiluminescence kit (Millipore) was used to detect the targeted protein. The specific antibodies used in our study are summarized in **Supplementary Table 2**.

### 2.9 Immunofluorescence Staining

Transfected cells ( $1 \times 10^5$ ) were cultured in a 24-well plate. After 24 h, the cells were fixed in 4% paraformaldehyde for 15 min, permeabilized with 0.5% Triton X-100 for 10 min, blocked in goat serum (Yeasen) for 1.5 h, and incubated with primary antibodies at 4  $^{\circ}$ C overnight. The next day, fluorescence-labeled secondary antibody was used to label the target protein in the cells, and 4',6-diamidino-2-phenylindole (Yeasen) was used to stain the cell nucleus according to the manufacturer's instructions. Fluoromount-G $^{\text{TM}}$  (Yeasen) was used to prevent fluorescence quenching, and the results were recorded using an inverted fluorescent microscope (IX51; Olympus, Tokyo, Japan). All antibodies used are summarized in **Supplementary Table 2**.

### 2.10 Wound Healing Assay

When the transfected cells reached 80–90% confluence in a 6-well plate, a 200  $\mu$ L sterilized pipette tip was used to create a scratch. The pipette tip was held perpen-

dicular to the bottom of the plate and moved along the lines previously marked on the back of the plate with a marker pencil. After creating the scratch, the cells were washed three times with phosphate-buffered saline (PBS), and then 2 mL serum-free DMEM was added for further incubation at 37 °C. The width of the scratch was measured at 0 and 24 h. The wound healing rate during the 24 h was calculated to assess the mobility changes of the SKOV3 cells.

### 2.11 Transwell Migration and Invasion Assay

For the migration assay, a Transwell with 8.0 μm pore membrane inserts (BD Biosciences, Franklin Lakes, NJ, USA) was placed in the well of a 24-well plate. Approximately  $1 \times 10^5$  transfected cells suspended in 200 μL serum-free DMEM were seeded into the upper chamber, while 400 μL DMEM containing 10% FBS was added to the space between the chamber and the bottom of the well. Then the 24-well plate was incubated in a 37 °C incubator for 24 h. A cotton swab was used to remove the non-migrated cells. The chamber was subsequently immersed in 4% paraformaldehyde for 20 min to fix the cells. Following fixation, the cells were stained with 0.1% crystal violet (Beyotime, Beijing, China) for 20 min. Excess crystal violet was washed away with PBS, and the results were recorded. The invasion assay followed a similar procedure as the migration assay, with the only difference being that the invasion chamber was coated with Matrigel (Corning, Shanghai, China) diluted in serum-free medium.

### 2.12 Vascular Mimicry (VM)

The Matrigel (Corning) was diluted in an equal volume of serum-free medium, added to a 21-well plate (200 μL/well) to form a thick gel, and then incubated at 37 °C for 2 h. Approximately  $1 \times 10^5$  transfected cells were seeded on top of the gel and cultured for 4 h before recording the results.

### 2.13 Cell Proliferation Assay

About 3000 SKOV3 cells were cultured in a 96-well plate for 24 h. Then the same concentrations of siRIPK4 and siNC were transfected using an siRNA reagent system (Biogen) according to the manufacturer's instructions. After transfection, 10 μL Cell Counting Kit-8 Reagent (Dalian Meilun Biotechnology, Dalian, China) was added to each well and incubated for 2 h at 37 °C to measure the absorbency reflecting cellular viability at 0, 24, and 48 h.

### 2.14 Cell Apoptosis Assay (Annexin V/Propidium Iodide)

Approximately  $1 \times 10^5$  transfected cells were harvested to determine the rates of cell apoptosis. The harvested cells were washed twice with chilled PBS and subsequently stained using the Annexin V/PI Apoptosis Detection Kit (Yeasen) following the manufacturer's instructions. After filtration, the cell suspension was analyzed using the CytoFLEX S Flow Cytometer (Beckman Coulter, Brea, CA, USA).

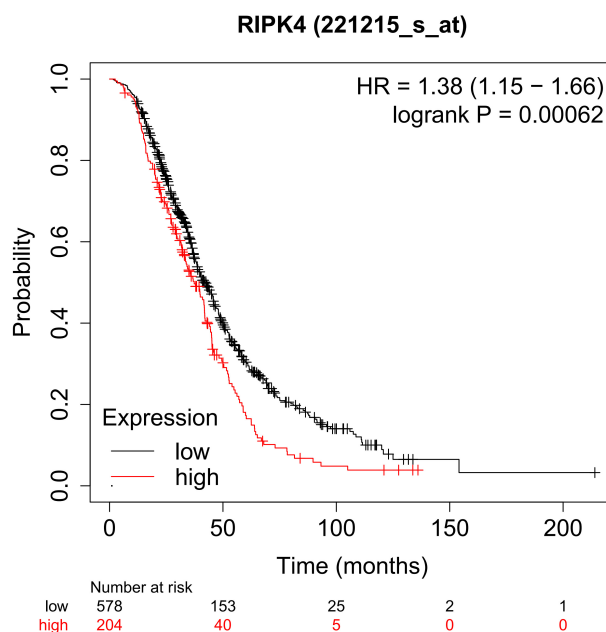


**Fig. 2. Relationship between RIPK4 expression and post-progression survival.**

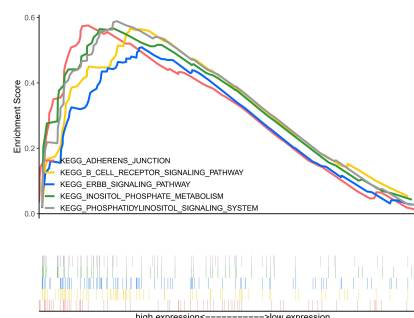


**Fig. 3. Relationship between RIPK4 expression and signaling pathways using gene set enrichment analysis (GSEA).**

### 2.15 Subcutaneous Xenografts in Nude Mice

All female nude mice used in this study were obtained from Xiamen University Laboratory Animal Center when they were approximately 4–6 weeks old. Before the start of the animal experiment, the mice were housed in a specific pathogen-free (SPF) clean-level environment for 1 week. To establish the xenograft model, approximately  $2 \times 10^6$  SKOV3 cells suspended in 200 μL PBS and transfected with either siNC or siRIPK4 were injected into the right skin of the back of the neck of the nude mice. After 6 weeks, the volume of subcutaneous xenografts was measured using the formula: volume = length  $\times$  width<sup>2</sup>/2.

**Table 1. Patient's clinical features by RIPK4 status in OC patients.**

Variables	n	RIPK4 status		p
		Low expression (%)	High expression (%)	
Age (years) (n = 373)				
<53	111	62 (31.6)	49 (27.7)	0.078
≥53	262	134 (68.4)	128 (72.3)	
FIGO stage (n = 370)				
II	30	12 (6.2)	9 (5.1)	0.017
III	292	162 (83.5)	130 (73.9)	
IV	57	20 (10.3)	37 (21.0)	
Tumor grade (n = 372)				
2	42	23 (11.9)	19 (11.2)	0.842
3	320	170 (88.1)	150 (88.8)	
Lymphatic invasion (n = 147)				
No	47	27 (34.6)	20 (29.0)	0.465
Yes	100	51 (65.4)	49 (71.0)	

RIPK4, receptor-interacting protein kinase 4; FIGO, Federation International of Gynecology and Obstetrics.

### 2.16 Intraperitoneal Xenograft in Nude Mice

All female nude mice used in our study were obtained from Xiamen University Laboratory Animal Center. They were approximately 4–6 weeks old and were kept in an SPF-clean level environment for 1 week before prior to initiation of the animal experiments. For the experiment, approximately  $2 \times 10^6$  SKOV3 cells suspended in 200  $\mu$ L PBS and transfected with either siNC or siRIPK4 were injected into the abdominal cavity of the nude mice. After 6 weeks, the abdominal circumference of the nude mice was measured, and the size of the heterotopic xenograft resulting from intraperitoneal injection was determined. The tumor xenografts were removed, photographed, weighed, and fixed for further analyses.

### 2.17 Immunohistochemical Staining

The tissue was fixed in 4% polyformaldehyde at 4 °C overnight, followed by gradient ethanol dehydration, clearing with xylene, and paraffin embedding to create paraffin specimens. The paraffin specimens were cut into 4  $\mu$ m thick wax sections for immunohistochemical staining. EDTA antigen repair solution (Solarbio) was used for antigen retrieval (95 °C for 10 min), and the tissue was cycled using an immunohistochemical pen. The Ultra Sensitive TM SP (Mouse/Rabbit) IHC Kit (Maxim Biotechnologies, Fuzhou, China) was used for immunohistochemical staining following the manufacturer's instructions. The tissue sections were visualized using the Enhanced HRP-DAB Kit (Maxin) under the Olympus IX51 microscope (Olympus, Tokyo, Japan).

### 2.18 Statistical Analysis

All data were analyzed using IBM SPSS Statistics 22 software (IBM Corp., Armonk, NY, USA). The experiment was conducted in triplicate, and the results are pre-

**Table 2. Multivariate survival analysis of overall survival in OC patients.**

Variables	HR	95% CI	p
Age (years)			
<53	1		0.011
≥53	1.509	1.101–2.067	
RIPK4 status			
Low expression	1	1	0.003
High expression	1.500	1.147–1.963	

HR, hazard ratio; CI, confidence interval; RIPK4, receptor-interacting protein kinase 4.

sented as the mean  $\pm$  standard deviation. Student's *t*-test and one-way analysis of variance (ANOVA) data were used for statistical analyses. The categorical variables for low and high expression of RIPK4 were compared using chi-squared tests, and the results were further validated using one-way ANOVA with Bonferroni's post hoc test.  $p < 0.05$  was considered statistically significant.

## 3. Results

### 3.1 RIPK4 Is Overexpressed in OC

GEPIA was utilized to compare the mRNA expression of RIPK4 in 426 serous OC tissues and 88 normal ovarian tissues. The results showed a significant increase in RIPK4 expression in serous OC compared to normal ovarian tissues (Fig. 1A). According to the Oncomine database, RIPK4 was also overexpressed in serous adenocarcinoma, mucinous adenocarcinoma, and clear cell adenocarcinoma compared with normal ovarian tissues (Fig. 1B). Fig. 1C shows the distinct expression patterns of RIPK4 across various cancers and their corresponding normal tissues. More-

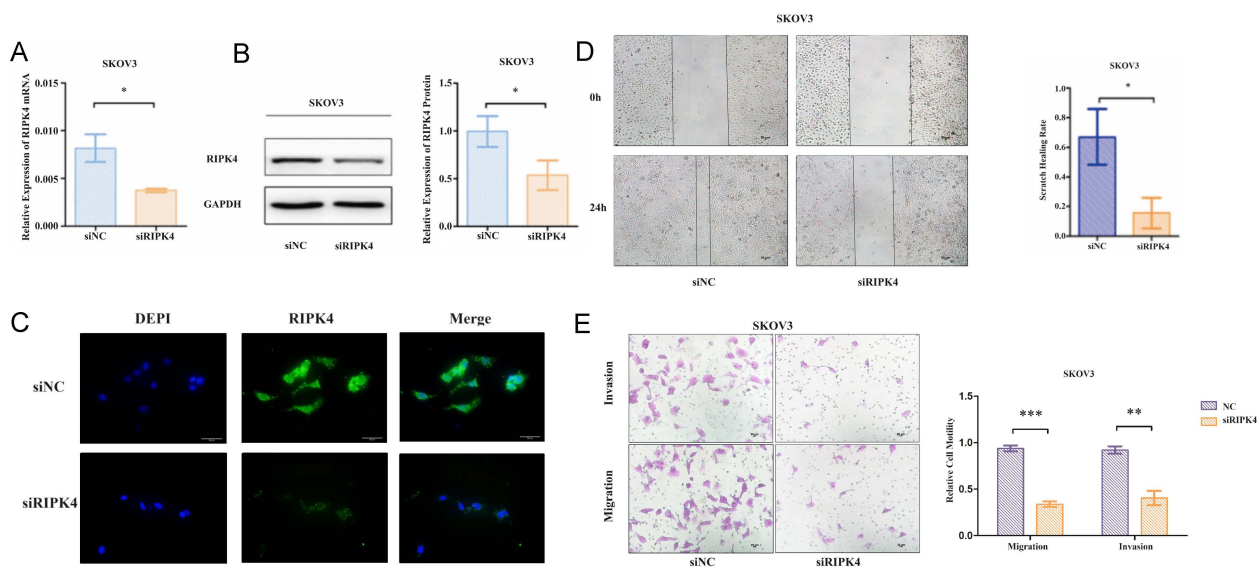


**Fig. 4. Silencing of RIPK4 inhibits the migration and invasion abilities of OC cells.** (A–C) qPCR, WB, and immunofluorescence staining were performed to assess the expression of RIPK4 in SKOV3 cells after transfection with siRIPK4 or siNC. (D,E) Silencing of RIPK4 suppressed the mobility of SKOV3 as demonstrated by the wound healing assay and transwell invasion and migration assays. The data are presented as the mean  $\pm$  SD, and statistical significance is indicated as follows: \* $p < 0.05$ , \*\* $p < 0.01$ , and \*\*\* $p < 0.001$ . qPCR, quantitative PCR; WB, western blotting.

over, immunohistochemical staining of clinical samples confirmed the overexpression of RIPK4 in serous OC tissue compared to normal ovarian tissue (Fig. 1D).

### 3.2 RIPK4 Is Overexpressed in Advanced-Stage OC

From TCGA database, the status of RIPK4 was divided into two groups: high-expressing RIPK4 (47.3%) and low-expressing RIPK4 (52.7%). The results revealed a significant association between the level of RIPK4 expression and the clinical stage of the patients. Patients with stage IV disease exhibited a significantly higher level of RIPK4 expression compared to those with early stage disease ( $p = 0.017$ ). These results were further supported by one-way ANOVA with Bonferroni's post hoc test ( $p = 0.013$ ), which also indicated a significant difference in RIPK4 expression between the two groups ( $p = 0.013$ ). However, no significant associations were observed between the expression of RIPK4 and age, tumor grade, and lymphatic invasion (Table 1).

### 3.3 Overexpression of RIPK4 Affects the Prognosis of OC

Using the data from TCGA database, multivariate survival analysis showed that high expression of RIPK4 was independently associated with worse overall survival compared to low RIPK4 expression (hazard ratio [HR]: 1.500;

95% confidence interval [CI]: 1.147–1.963;  $p = 0.003$ ) (Table 2). Findings from the KM plotter database also showed that high RIPK4 expression was associated with poorer post-progression survival compared to low RIPK4 expression (HR: 1.38, 95% CI: 1.15–1.66;  $p = 0.00062$ ) (Fig. 2).

### 3.4 GSEA of RIPK4 in OC

The results of GSEA analysis indicated that RIPK4 might be associated with several signaling pathways including the cell adhesion, B-cell receptor, ERBB, inositol phosphate metabolism, and phosphatidylinositol signaling pathways. Among these pathways, cell adhesion was found to be most significant (Fig. 3).

### 3.5 Suppression of RIPK4 Inhibits the Migration and Invasion of OC Cells in Vitro

The SKOV3 cell line was utilized to establish a cell model with low RIPK4 expression by transfecting siRIPK4 or siNC to further explore the role of RIPK4 in OC [11]. The expression of RIPK4 was assessed using qPCR, WB, and immunofluorescence. The findings demonstrated that specific siRNA effectively reduced the expression of RIPK4 (Fig. 4A–C). Furthermore, wound healing and Transwell migration/invasion experiments were conducted to evaluate the effect of RIPK4 on the mobility of OC

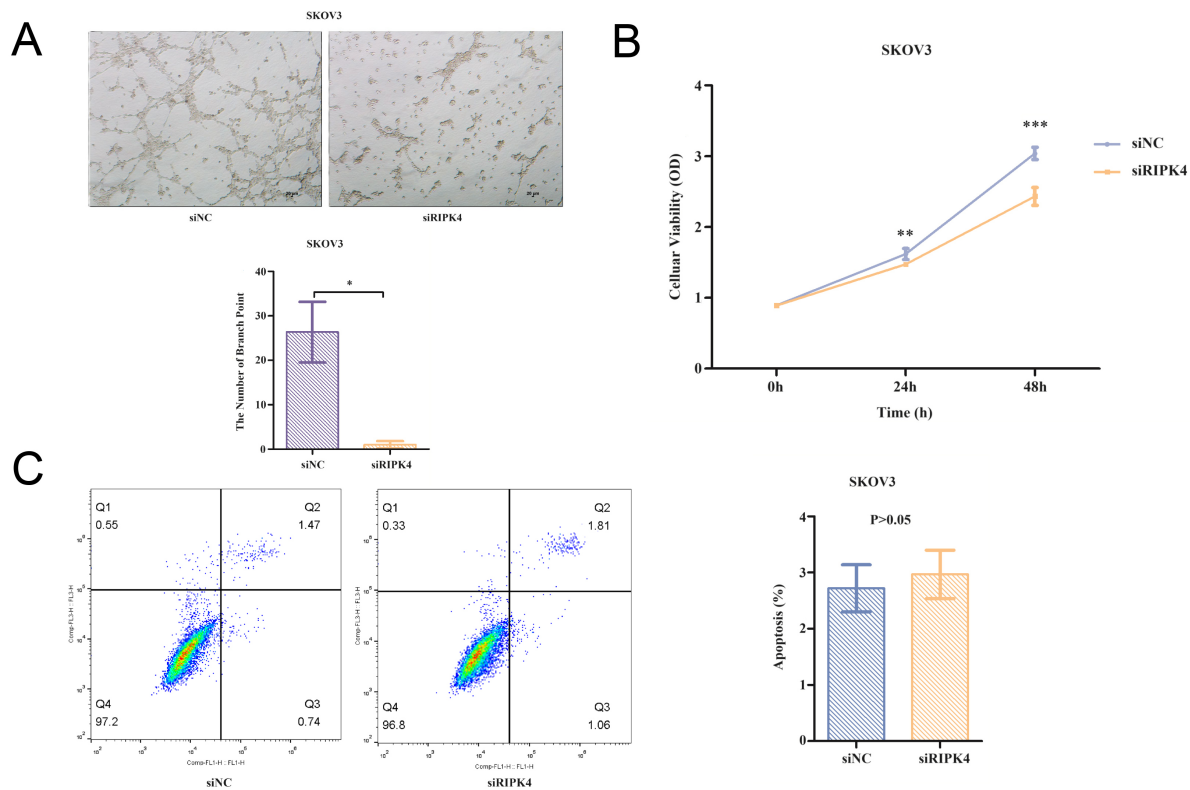


**Fig. 5. Inhibition of RIPK4 suppresses the vascular mimicry (VM) and growth of OC cells.** (A) Suppression of RIPK4 expression resulted in the reduced VM of SKOV3 cells by culturing in Matrigel. (B) Suppression of RIPK4 expression inhibited the growth of SKOV3 cells assessed by the Cell Counting Kit-8 assay. (C) Suppression of RIPK4 expression did not significantly affect the apoptosis of SKOV3 cells by Annexin V/propidium iodide (PI) staining. The data are presented as the mean  $\pm$  SD, and statistical significance is indicated as follows: \* $p < 0.05$ , \*\* $p < 0.01$ , and \*\*\* $p < 0.001$ .

cells. The results indicated that the down-regulation of RIPK4 suppressed the metastasis and invasion of OC cells (Fig. 4D,E).

### 3.6 Suppression of RIPK4 Inhibits the VM of OC Cells in Vitro

The concept of VM is that malignant tumor cells can form a circular pipeline network similar to blood vessels, providing nutrition to the tumors. VM has also been investigated in OC [12]. *In vitro* experiments using three-dimensional matrigel culture were conducted to investigate the effect of RIPK4 on VM formation in OC cells. The results demonstrated that the downregulation of RIPK4 significantly inhibited the formation of circular pipeline structures, indicating that suppression of RIPK4 could also inhibit the vasculogenic mimicry of OC cells (Fig. 5A).

### 3.7 Suppression of RIPK4 Inhibits the Growth of OC Cells in Vitro

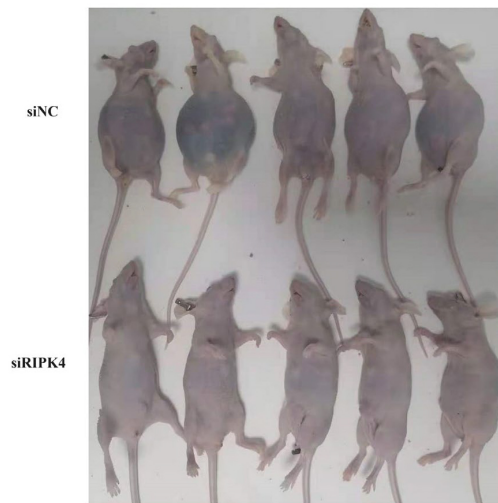
The CCK8 reagent was used to assess the role of RIPK4 in cellular growth. The results demonstrated that the downregulation of RIPK4 significantly inhibited the growth of OC cells (Fig. 5B). However, there was no significant ef-

fect on the apoptosis of OC cells in the RIPK4-knockdown group using the cellular apoptosis assay (Fig. 5C). Moreover, the results of subcutaneous xenografts in nude mice showed that the volume of subcutaneous xenografts in the negative control group was bigger than that in the RIPK4-knockdown group, although the difference was not statistically significant (Supplementary Fig. 1).

### 3.8 Suppression of RIPK4 Inhibits the Growth of Intraperitoneal Xenograft in Nude Mice

The growth of abdominal tumors was significantly inhibited in nude mice injected with SKOV3 cells transfected with siRIPK4 compared with the siNC group (Fig. 6A). Moreover, a greater number of xenografts was found to be spreading extensively in the abdominal cavity of nude mice in the siNC group, invading nearly all areas of the intestinal curvature. However, the spread of xenografts was limited in the RIPK4-knockdown group, with only a few abdominal peritoneal nodules with or without slight intestinal curvature invasion observed (Fig. 6B). Therefore, the suppression of RIPK4 may have the potential to inhibit the intraabdominal spread of OC.

A



B



**Fig. 6. Silencing RIPK4 inhibits the growth of intraperitoneal xenograft in nude mice.** (A) Silencing of RIPK4 significantly reduces abdominal enlargement in nude mice following intraperitoneal injection of SKOV3 cells. (B) Heterotopic xenografts were surgically removed, visually inspected, and weighed from each nude mouse at 6 weeks after intraperitoneal injection. The data are presented as the mean  $\pm$  SD, and statistical significance is indicated as follows: \*\*\* $p < 0.001$ .

### 3.9 Suppression of RIPK4 Inhibits the EMT in OC

EMT is a critical biological process that enables epithelial-derived cancer cells to undergo migration and invasion. qPCR and WB were used to investigate the role of RIPK4 in regulating EMT. The results demonstrated that the downregulation of RIPK4 led to a significant increase in expression of the epithelial marker E-cadherin while decreasing expression of the mesenchymal marker N-cadherin. However, RIPK4 downregulation only slightly suppressed the transcription of the vimentin gene ( $p < 0.05$ ) and did not affect expression of the vimentin protein. Moreover, there was no noticeable impact on the expression of Twist mRNA and protein (Fig. 7A,B). Furthermore, *in vitro* experiments using intraperitoneal xenograft tumors demonstrated that suppression of RIPK4 resulted in downregulation of N-cadherin and upregulation of E-

cadherin (Fig. 7C). Taken together, these findings indicate that RIPK4 primarily regulates the EMT in OC development by modulating the expression of E-cadherin and N-cadherin.

## 4. Discussion

In this study, we investigated the clinical role and biological function of RIPK4 in OC. Our findings revealed that RIPK4 was overexpressed in OC and had a significant impact on the survival of OC patients. Moreover, silencing of RIPK4 resulted in significant inhibition of intraperitoneal tumor growth, invasion, and VM of OC both *in vitro* and *in vivo*. Furthermore, RIPK4 was found to promote OC progression by inducing the EMT *in vitro*. These results suggest that RIPK4 has the potential to be a therapeutic target for OC.

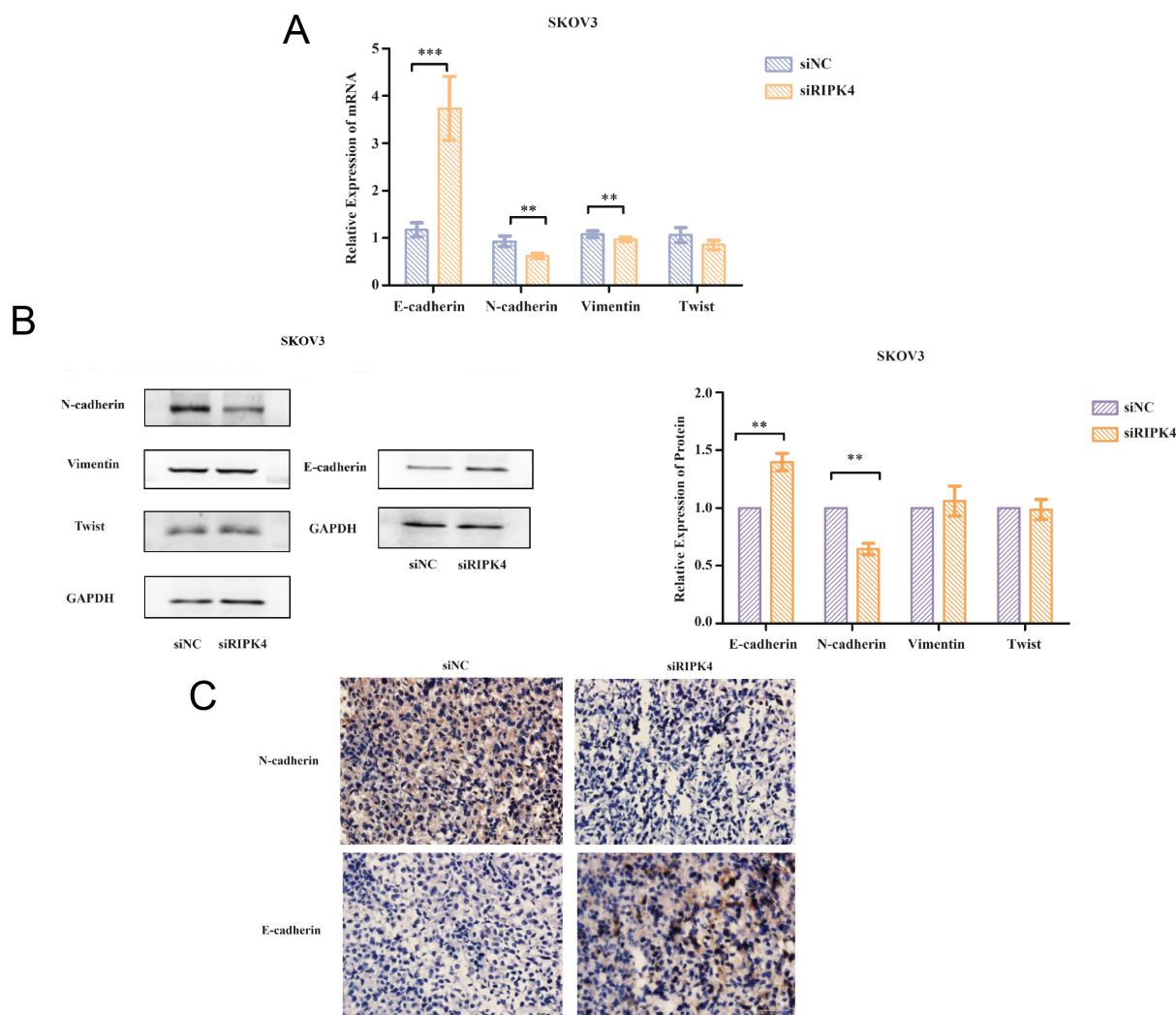


**Fig. 7. Silencing of RIPK4 inhibits the epithelial–mesenchymal transition (EMT) *in vitro* and *in vivo*.** (A,B) qPCR and WB were performed to assess the expression of EMT-related markers following transfection with siRIPK4 or siNC. (C) Immunohistochemical staining of EMT-related markers after transfection with siRIPK4 or siNC. The data are presented as the mean  $\pm$  SD, and statistical significance is indicated as follows: \*\* $p < 0.01$ , and \*\*\* $p < 0.001$ .

The clinical role of RIPK4 in OC was consistent with its role in other cancers such as bladder cancer [13], pancreatic cancer [14], nasopharyngeal carcinoma [15], cervical cancer [16], and osteosarcoma [17]. However, RIPK4 may act as a tumor suppressor gene in other cancers including skin squamous cell carcinoma [18], esophageal squamous cell carcinoma [19], tongue squamous cancer [20], lung adenocarcinoma [21], and hepatocellular carcinoma [22]. The different roles of RIPK4 in various tumors may be related to its heterogeneous characteristics and ability to regulate different signaling pathways. For example, RIPK4 activates Wnt/ $\beta$ -catenin, which is associated with the development of various malignancies [7]. In bladder cancer [13] and nasopharyngeal carcinoma [15], RIPK4 activates the nuclear factor kappa B/vascular endothelial growth factor signaling pathway to promote the metastasis of can-

cer cells. However, RIPK4 activates plakophilin 1 in keratinocytes and inhibits the extracellular signal-regulated pathway, leading to an increased incidence of skin cancer [23].

In our study, the results of GSEA showed that RIPK4 may be associated with cell adhesion, which plays a critical role in the metastasis of tumor cells. Moreover, functional studies have demonstrated that downregulation of RIPK4 inhibits invasion, metastasis, and intraperitoneal tumor growth in OC cells. The EMT is a key mechanism regulating the implantation and metastasis of OC, primarily through cell adhesion molecules, especially the cadherin family [24,25]. Several previous studies have also shown that RIPK4 can regulate migration and invasion in various cancers by inducing the EMT [13,15–17]. In our study, we observed that RIPK4 can regulate the EMT by altering the

expression of N-cadherin and E-cadherin both *in vitro* and *in vivo*. Moreover, the Wnt/ $\beta$ -catenin pathway, which can be activated by RIPK4, has been identified as an important signaling pathway in regulating the EMT in OC [7,26].

VM is a process in which tumor cells mimic the formation of blood vessels, providing nutrition for malignancies [27,28]. Our study revealed that RIPK4 has a positive effect on the formation of VM in OC cells, which is associated with a poor prognosis in OC patients [27,28]. Mechanically, the EMT has also been linked to VM in OC through the regulation of Twist1 expression [24]. However, our results showed that Twist1 was not regulated by RIPK4, suggesting the involvement of another pathway in RIPK4-mediated VM formation.

While several studies have demonstrated that suppression of RIPK4 inhibits subcutaneous tumor growth of cervical cancer [16] and osteosarcoma [17], our study did not find significant differences in subcutaneous xenografts between RIPK4-knockdown and siNC groups. However, we found that the suppression of RIPK4 inhibited the growth of intraperitoneal xenografts in nude mice. Ascite formation is one of the critical pathways for OC invasion, and our findings suggest that suppression of RIPK4 may inhibit the intraabdominal spread of OC. Further investigations are needed to explore the impact of RIPK4 expression on ascite formation in OC patients.

This study had several limitations. First, we only used the SKOV3 cell line; thus, additional studies using multiple OC cell lines are required to validate our findings. Second, there is a lack of clinical evidence to verify the association between RIPK4 and intraabdominal metastasis in OC patients. Third, the molecular mechanism of RIPK4 regulating the biological behavior of OC needs to be further investigated. Finally, we did not use *in vivo* models to study the relationship among overall survival rate, tumor stage, and RIPK4 expression.

## 5. Conclusion

In conclusion, the results of our study suggest that RIPK4 may function as an oncogene in the development and prognosis of OC. Further exploration is needed to elucidate the specific molecular mechanisms underlying the role of RIPK4 and its potential application in the diagnosis or treatment of OC.

## Availability of Data and Materials

The data sets generated and/or analyzed during the current study are available in the GEPIA database (<http://gepia.cancer-pku.cn/>), Oncomine database (<https://www.oncomine.org>), TCGA (<https://www.tcg.org/>), and KM plotter database (<http://www.kmplot.com/analysis/>). Data from non-database sources are available from the corresponding author upon reasonable request.

## Author Contributions

LH, JHW, and JYX drafted the manuscript. LH acquired the datasets. JZ and SGW conceived the study. LH and JYX conducted the statistical analyses. JYX, JHW, LH, SGW, and JZ participated in the study design. All authors read and approved the final manuscript. All authors contributed to editorial changes in the manuscript. All authors have participated sufficiently in the work and agreed to be accountable for all aspects of the work.

## Ethics Approval and Consent to Participate

All human and animal protocols described in this study were approved by the Ethics Committee of the First Affiliated Hospital of Xiamen University for all human or animal experimental investigations (approval no. 2021GGB027).

## Acknowledgment

Not applicable.

## Funding

This work was partly supported by grants from the Natural Science Foundation of Fujian Province (No. 2022J011379) and the Commission Young and Middle-aged Talents Training Project of Fujian Health Commission (No. 2021GGB027).

## Conflict of Interest

Given her role as Guest Editor, Juan Zhou had no involvement in the peer-review of this article and has no access to information regarding its peer-review. Full responsibility for the editorial process for this article was delegated to Mariafrancesca Cascione. The authors declare no conflict of interest.

## Supplementary Material

Supplementary material associated with this article can be found, in the online version, at <https://doi.org/10.31083/j.fbl2812368>.

## References

- [1] Maringe C, Walters S, Butler J, Coleman MP, Hacker N, Hanna L, *et al.* Stage at diagnosis and ovarian cancer survival: evidence from the International Cancer Benchmarking Partnership. *Gynecologic Oncology*. 2012; 127: 75–82.
- [2] Zuna RE. Diagnostic Cytopathology of Peritoneal Washings. *CytoJournal* 2022; 19: 9.
- [3] Wu SG, Wang J, Sun JY, He ZY, Zhang WW, Zhou J. Real-World Impact of Survival by Period of Diagnosis in Epithelial Ovarian Cancer Between 1990 and 2014. *Frontiers in Oncology*. 2019; 9: 639.
- [4] Dao F, Schlappe BA, Tseng J, Lester J, Nick AM, Lutgendorf SK, *et al.* Characteristics of 10-year survivors of high-grade serous ovarian carcinoma. *Gynecologic Oncology*. 2016; 141: 260–263.

- [5] Oberbeck N, Pham VC, Webster JD, Reja R, Huang CS, Zhang Y, *et al.* The RIPK4-IRF6 signalling axis safeguards epidermal differentiation and barrier function. *Nature*. 2019; 574: 249–253.
- [6] Xu J, Wei Q, He Z. Insight Into the Function of RIPK4 in Keratinocyte Differentiation and Carcinogenesis. *Frontiers in Oncology*. 2020; 10: 1562.
- [7] Huang X, McGann JC, Liu BY, Hannoush RN, Lill JR, Pham V, *et al.* Phosphorylation of Dishevelled by protein kinase RIPK4 regulates Wnt signaling. *Science (New York, N.Y.)*. 2013; 339: 1441–1445.
- [8] Tang Z, Li C, Kang B, Gao G, Li C, Zhang Z. GEPIA: a web server for cancer and normal gene expression profiling and interactive analyses. *Nucleic Acids Research*. 2017; 45: W98–W102.
- [9] Rhodes DR, Yu J, Shanker K, Deshpande N, Varambally R, Ghosh D, *et al.* ONCOMINE: a cancer microarray database and integrated data-mining platform. *Neoplasia (New York, N.Y.)*. 2004; 6: 1–6.
- [10] Nagy Á, Lániczky A, Menyhart O, Györfy B. Validation of miRNA prognostic power in hepatocellular carcinoma using expression data of independent datasets. *Scientific Reports*. 2018; 8: 9227.
- [11] Hua W, Christianson T, Rougeot C, Rochefort H, Clinton GM. SKOV3 ovarian carcinoma cells have functional estrogen receptor but are growth-resistant to estrogen and antiestrogens. *The Journal of Steroid Biochemistry and Molecular Biology*. 1995; 55: 279–289.
- [12] Ayala-Domínguez L, Olmedo-Nieva L, Muñoz-Bello JO, Contreras-Paredes A, Manzo-Merino J, Martínez-Ramírez I, *et al.* Mechanisms of Vasculogenic Mimicry in Ovarian Cancer. *Frontiers in Oncology*. 2019; 9: 998.
- [13] Liu JY, Zeng QH, Cao PG, Xie D, Chen X, Yang F, *et al.* RIPK4 promotes bladder urothelial carcinoma cell aggressiveness by upregulating VEGF-A through the NF- $\kappa$ B pathway. *British Journal of Cancer*. 2018; 118: 1617–1627.
- [14] Qi ZH, Xu HX, Zhang SR, Xu JZ, Li S, Gao HL, *et al.* RIPK4/PEBP1 axis promotes pancreatic cancer cell migration and invasion by activating RAF1/MEK/ERK signaling. *International Journal of Oncology*. 2018; 52: 1105–1116.
- [15] Gong Y, Luo X, Yang J, Jiang Q, Liu Z. RIPK4 promoted the tumorigenicity of nasopharyngeal carcinoma cells. *Biomedicine & Pharmacotherapy*. 2018; 108: 1–6.
- [16] Liu DQ, Li FF, Zhang JB, Zhou TJ, Xue WQ, Zheng XH, *et al.* Increased RIPK4 expression is associated with progression and poor prognosis in cervical squamous cell carcinoma patients. *Scientific Reports*. 2015; 5: 11955.
- [17] Yi Z, Pu Y, Gou R, Chen Y, Ren X, Liu W, *et al.* Silencing of RIPK4 inhibits epithelial-mesenchymal transition by inactivating the Wnt/ $\beta$ -catenin signaling pathway in osteosarcoma. *Molecular Medicine Reports*. 2020; 21: 1154–1162.
- [18] Poligone B, Gilmore ES, Alexander CV, Oleksyn D, Gillespie K, Zhao J, *et al.* PKK suppresses tumor growth and is decreased in squamous cell carcinoma of the skin. *The Journal of Investigative Dermatology*. 2015; 135: 869–876.
- [19] Li XC, Wang MY, Yang M, Dai HJ, Zhang BF, Wang W, *et al.* A mutational signature associated with alcohol consumption and prognostically significantly mutated driver genes in esophageal squamous cell carcinoma. *Annals of Oncology: Official Journal of the European Society for Medical Oncology*. 2018; 29: 938–944.
- [20] Wang X, Zhu W, Zhou Y, Xu W, Wang H. RIPK4 is downregulated in poorly differentiated tongue cancer and is associated with migration/invasion and cisplatin-induced apoptosis. *The International Journal of Biological Markers*. 2014; 29: e150–e159.
- [21] Koppam J, Chiffelle J, Angelino P, Piersigilli A, Zangger N, Delorenzi M, *et al.* RIP4 inhibits STAT3 signaling to sustain lung adenocarcinoma differentiation. *Cell Death and Differentiation*. 2017; 24: 1761–1771.
- [22] Li H, Luo D, Huttad L, Zhang M, Wang Y, Feng J, *et al.* RIPK4 Suppresses the Invasion and Metastasis of Hepatocellular Carcinoma by Inhibiting the Phosphorylation of STAT3. *Frontiers in molecular biosciences*. 2021; 8: 654766.
- [23] Lee P, Jiang S, Li Y, Yue J, Gou X, Chen SY, *et al.* Phosphorylation of Pkp1 by RIPK4 regulates epidermal differentiation and skin tumorigenesis. *The EMBO Journal*. 2017; 36: 1963–1980.
- [24] Zhu QQ, Ma C, Wang Q, Song Y, Lv T. The role of TWIST1 in epithelial-mesenchymal transition and cancers. *Tumour Biology: the Journal of the International Society for Oncodevelopmental Biology and Medicine*. 2016; 37: 185–197.
- [25] Vergara D, Merlot B, Lucot JP, Collinet P, Vinatier D, Fournier I, *et al.* Epithelial-mesenchymal transition in ovarian cancer. *Cancer Letters*. 2010; 291: 59–66.
- [26] Teeuwssen M, Fodde R. Wnt Signaling in Ovarian Cancer Stemness, EMT, and Therapy Resistance. *Journal of Clinical Medicine*. 2019; 8: 1658.
- [27] Liang J, Yang B, Cao Q, Wu X. Association of Vasculogenic Mimicry Formation and CD133 Expression with Poor Prognosis in Ovarian Cancer. *Gynecologic and Obstetric Investigation*. 2016; 81: 529–536.
- [28] Jiang J, Chen Y, Zhang M, Zhou H, Wu H. Relationship between CD177 and the vasculogenic mimicry, clinicopathological parameters, and prognosis of epithelial ovarian cancer. *Annals of Palliative Medicine*. 2020; 9: 3985–3992.